Ultrathin Chromia on a Hexagonally-Ordered d⁰ Ferromagnet: Magnetic Ordering and Interfacial Exchange Bias for Cr₂O₃/TiO_{2-x}/Al₂O₃(0001) at and above Room Temperature

Chad Ladewig¹, Fatima Anwar¹, Veronica Lee¹, Jeffery A. Kelber^{1*}, Syed Q. A. Shah², Peter A. Dowben²

Abstract

Heterostructures consisting of 1 nm thick chromia films and 5 nm thick titania films display significant exchange bias at and above room temperature. Chromia films ~ 1 nm thick were deposited by molecular beam epitaxy (MBE) of Cr in ultra-high vacuum at room temperature on 5 nm thick TiO2-x(111) films (x < 0.3) deposited epitaxially by MBE on Al2O3(0001). Cr deposition yields Ti(III) and Cr(III) formation without Cr/Ti interfacial mixing, as determined by in situ photoelectron spectroscopy (XPS) and electron energy loss spectroscopy (EELS). In situ low energy electron diffraction (LEED) data indicate hexagonally-ordered chromia. Planar and polar Magneto-optic Kerr Effect (MOKE) measurements at 300 K exhibit strong magnetic interaction between the boundary layer magnetization of chromia and the ferromagnetic substrate. These data demonstrate the robust room temperature interaction of the boundary layer magnetism of a multiferroic antiferromagnet with a d⁰ ferromagnetic substrate—a system with strong potential for voltage-switchable spintronic devices.

Keywords: d⁰ ferromagnetism; magneto-electric antiferromagnet; Magnéli phase; magneto-optic Kerr effect; photoemission

1. Introduction

The exploitation of room temperature dilute magnetic semiconductors, including d^0 ferromagnets such as titania, for spintronic applications is of long standing interest [1-3], and the coupling of such materials with a voltage-switchable antiferromagnet, such as chromia, presents an avenue toward low-power, non-volatile memory and logic applications [4]. Previous studies, however, have demonstrated that magnetic performance can be adversely affected by factors not completely understood, but which may include interfacial Cr/Ti mixing [1], and possibly poor control of O vacancies resulting in magnetic ordering only at T < 50 K [5]. Importantly, such studies have generally involved either rutile or anatase forms of TiO₂ [1, 3, 5].

In contrast, here we present data for ultra-thin Cr_2O_3 films deposited on titania films of unusual structure and composition: $TiO_{2-x}(111)$ films (x<0.3) grown epitaxially on $Al_2O_3(0001)$ substrates. The evidence here suggests that these are in fact Magnéli phases, similar to films grown on Pt(111) [6, 7] or Pt3Ti(111) [8]. Concentrations of oxygen vacancies in such films can, as shown below, be minimized by annealing in O_2 without loss of hexagonal order. Subsequent Cr deposition at room temperature results in additional O vacancy formation in the TiO_{2-x} substrate near the interface, which can enhance the d^0 ferromagnetic moment [3]. Such vacancies survive subsequent room temperature exposure of the chromia/titania interface to high

-

¹ Dept. of Chemistry, University of North Texas, Denton TX 76203

² Dept. of Physics and Astronomy, University of Nebraska-Lincoln, Lincoln, NE 68588

^{*} Jeffry.Kelber@unt.edu

O₂ pressures. The observation of strong exchange bias is evidence of antiferromagnetic/ferromagnetic coupling to at least 315 K, suggesting a straightforward route toward the formation of robust, voltage-switchable spintronic devices.

2. Experiment

Film deposition and characterization studies were carried out in a multi-chamber system with capabilities for molecular beam epitaxy (MBE), XPS, Auger electron spectroscopy (AES) and EELS, as described previously [9]. Al₂O₃(0001) substrates were cleaned by annealing in 10⁻⁶ Torr O₂ until LEED and XPS showed an ordered, carbon-free alumina surface. Ti deposition on Al₂O₃(0001) was carried out in a background of 10⁻⁶ Torr O₂ at 500 K and at an average deposition rate of 10 Å-min⁻¹. Cr deposition was carried out at room temperature and 1 x 10⁻⁹ Torr, at a rate of 1 Å-min⁻¹.

Titania films were deposited in a sequence of alternating deposition and annealing in a background of 10^{-6} Torr O_2 at 1000 K. (see Supplemental data, Fig. S1). O/Ti stoichiometry was estimated from the Ti(IV)/Ti(III) ratios obtained from deconvolution of the Ti 2p XPS spectra. This method is obviously approximate and ignores potential, albeit minor, contributions from other Ti oxidation states, but was necessitated by the fact that the titania films were sufficiently thin (~ 50 Å or less) as to allow significant contributions from the alumina substrate to the total O 1s XPS signal. This is apparent from the estimations of film stoichiometry based on relative O 1s and Ti 2p intensities (Supplemental data, Fig. S2). Using this method, O/Ti atomic ratios > 2 are observed for all films, although the ratios decreased exponentially with film thickness. This effect is consistent with a calculated [10] O 1s photoelectron inelastic mean free path of 20.2 Å through stoichiometric TiO2.

In situ XPS and EELS spectra were acquired using a commercial double pass cylindrical mirror analyzer (Staib) with co-axial electron gun. For EELS spectra, a 100 eV electron beam was used to maintain surface sensitivity. For XPS spectra, an unmonochromatized AlKα source (Physical Electronics) was used. The energy scale for XPS spectra was calibrated by setting the O 1s peak binding energy for clean Al₂O₃(0001) at 531.0 eV [11]. Core level XPS intensities, estimations of film thickness and spectral deconvolution were carried out by standard methods [10, 12], using commercially available software. For deconvolution of Ti 2p spectra, Gaussian-Lorentzian peaks were used, with FWHM of 3.0 eV, based on results for stoichiometric TiO₂ obtained with this analyzer. A Ti(IV)-Ti(III) 2p_{3/2} energy splitting of 1.4 eV was also used [13]. In-situ LEED images were obtained using a commercial reverse-view four grid LEED instrument (Omicron) with co-axial electron gun. MOKE measurements, with the magnetic field oriented both in-plane and out of the plane to the sample, were carried out using a custom built MOKE setup (Supplemental data Fig. S3). A 630 nm intensity-stabilized He-Ne laser beam was first linearly polarized and then passed from photoelastic modulator before interacting with the sample. For planar MOKE the beam was then incident on the sample at some acute angle with respect to normal. For polar MOKE, however, after passing from the photoelastic modulator, the beam was then passed from the beam splitter for the normal incident of beam on the sample. Reflection from the magnetic surface of chromia in the presence of applied field results in a change in the polarization angle of incident beam due to which a detectable change in beam intensity was recorded which is in accordance to Malus's law [14]. Before entering the photo detector this elliptically polarized beam is first passed from the analyzing polarizer. The MOKE

intensity is linked with the magnetization of the chromia sample and is plotted as a function of applied field.

3. Results

In-situ LEED data are displayed in Fig. 1 for (a) a clean $Al_2O_3(0001)$ surface; (b) a 5 nm thick $TiO_{1.8}(111)$ film on $Al_2O_3(0001)$; (c) a similar film as in (b), but annealed in O_2 to yield near-stoichiometric TiO_2 ; and (d) after Cr deposition at room temperature. Ti 2p XPS spectra corresponding to Figs. 1b-d are shown in Fig. 2a-c.

The results in Fig. 1 and Fig. 2 demonstrate that deposition of Ti films on Al₂O₃(0001) under these conditions results in hexagonally ordered titanium oxide films with significant Ti(III) content (e.g., TiO_{1.8}) and that extensive annealing in O₂ largely eliminates the observed Ti(III) component without apparent change in hexagonal orientation. The films with greater Ti(III) content were, as expected, more conductive, as indicated by the fact that titania films of all thicknesses, after annealing, exhibited significantly more charging in XPS. LEED spectra (Figs. 1c,d) were also impacted, with annealed films allowing image acquisition (albeit blurred) only at certain electron beam energies, and with the LEED electron beam in many instances migrating off the sample.

EELS spectra correlate with these results. O vacancies in titania yield electron occupancy of the Ti 3d states, and this is reflected in EELS spectra (Fig. 3) that indicate transitions at loss energies < 2 eV, consistent with electrons in mid-gap states and as expected for corundum-phase Ti₂O₃, for example [15]. Annealing in O₂ essentially eliminates Ti(III) components from Ti 2p XPS spectra (Fig. 2b), and also eliminates such low energy transitions from the EELS spectrum (Fig. 3b). However, as total film thicknesses increased, even films with substantial Ti(III) XPS spectral components exhibited significant charging in XPS, suggesting that the O vacancies were not uniformly distributed in the films.

The evolution of O 1s and Cr 2p XPS spectra upon Cr deposition are shown in Fig.4. O 1s spectra (Fig. 4a) exhibit considerable broadening toward higher binding energies upon chromia deposition, although the O 1s peak binding energy remains constant. Cr 2p spectra (Fig. 4b) exhibit no significant shift in binding energy with increasing thickness, indicating that Cr(III) is the predominant oxidation state throughout the Cr deposition process [16]. The O 1s broadening observed in Fig. 4a, however, is associated with the formation of O vacancies/non-lattice oxygen and OH groups in TiO₂ films [17].

These data are also consistent with the XPS Ti 2p spectrum (Fig. 2c) showing an increase in the deconvoluted Ti 2p Ti(III)/Ti(IV) intensity ratio upon Cr deposition. The data in Figs. 2 and 4, therefore, indicate the migration of O atoms from the titania substrate into the growing chrome overlayer during Cr metal deposition in UHV at room temperature. Cr deposition also results in a monotonic attenuation of the Ti 2p signal intensity relative to the O 1s signal intensity (Fig. 5). This is consistent with migration of O from titania into a Cr overlayer, but without significant Cr/Ti interfacial mixing. LEED spectra acquired after ~ 10 Å chromia formation (Fig. 1d) are blurred, but exhibit a hexagonal LEED pattern, consistent with formation of a (0001)-oriented film on top of the TiO_{2-x}(111) film. Thus, the data indicate formation of a hexagonally-ordered Cr₂O₃/TiO_{2-x} heterostructure. The titania oxygen vacancies are not readily passivated upon exposure to higher pressures of O₂. Exposure of this interface to ~ 10^{-4} Torr O₂ for 30 minutes at room temperature yielded no significant change in the relative Ti(III) intensity in the XPS Ti 2p signal (not shown).

Planar and polar MOKE data were acquired between 280 K and 315 K for the $Cr_2O_3/TiO_{2-x}(111)$ film, and showed little variation with temperature, exhibiting significant exchange bias and hysteresis. Planar MOKE data acquired at 300 K are displayed in Fig. 6a, and corresponding polar MOKE data at this temperature are shown in Fig. 6b. It can be seen in Figure 6a that the center of the hysteresis is translated from its normal center i.e. H = 0 to $HE \neq 0$. Exchange bias and some evidence of residual antiferromagnetism is evident in the polar MOKE taken at 300 K (Figure 6b), although exchange bias dominates in a manner similar to that seen in the planar MOKE results.

4. Discussion

The data presented here demonstrate strong chromia/titania interfacial magnetic interactions at and above room temperature, in direct contrast to previous reports indicating exchange bias at the $Cr_2O_3(10-10)$ /rutile-TiO2(001) interface only for T < 40 K [5]. This striking difference suggests—aside from an obvious difference in film orientation--significant differences in the nature of the TiO₂ substrate, and possibly in the way the chromia/titania interface is formed, with implications for future device applications.

Studies of TiO₂ growth on Al₂O₃(0001) at elevated deposition or annealing temperatures report formation of rutile TiO₂(001), albeit with the formation of a Ti₂O₃(111) interfacial layer ~ 1 nm thick [18]. The lattice constants for this corundum phase Ti₂O₃(111) layer are a = b = 5.1 Å [18]. A comparison of the LEED spectra in Figs. 1a, b indicates that the lattice constant of the TiO_{2-x}(111) film is 5.1 Å, in very good agreement with that of Ti₂O₃(111). That such films can be grown on top of similar films after extensive annealing in O₂ (Supplemental data, Fig. S1) indicates that annealing in O₂ does not significantly alter film lattice constants or orientation. These data therefore indicate that the TiO_{2-x}(111) films studied here are in fact Magnéli phases (Ti_nO_{2n-γ}). Similar, hexagonally ordered Magnéli phases of titania have been grown under similar deposition conditions on Pt(111) [6]. Additionally, brief room temperature exposures of such phases, including bulk Ti₂O₃, to O₂ or ambient, substantially reduces the number of O vacancies within the XPS sampling depth, yielding a nearly stoichiometric TiO₂ film according to XPS [19], in agreement with our results (Fig. 2). Therefore, the data in Figs. 1 and 2 indicate that the TiO_{2-x}(111) films examined here are in fact Magnéli phases, or, essentially, O-rich corundum phase Ti₂O₃.

Previous studies of chromia/titania interface formation at various temperatures moderately elevated above 300 K, have reported Cr/Ti intermixing [1, 20, 21] with quenching of magnetism, even at highly ordered interfaces. The data presented here, however, indicate that Cr deposition in UHV at room temperature results in O migration into the Cr overlayer, resulting in chromia formation and enhanced Ti(III) sites near the interface (Figs. 2, 3), but with negligible Cr/Ti interfacial mixing. Indeed, XPS data (Fig. 5) demonstrate that the O 1s/Ti 2p intensity ratio (with similar inelastic mean free paths for both O 1s and Ti 2p photoelectrons) increases with Cr deposition at room temperature, consistent with preferential attenuation of the Ti 2p intensity, due to O migration into the growing Cr overlayer. The stability of the Ti(III) sites thus formed upon exposure to relatively high pressures of O₂ suggests that this interface is relatively stable under ambient conditions, consistent with the ex situ MOKE data (Fig. 6).

LEED data (Fig. 1d) indicate that the chromia overlayer thus formed is hexagonally ordered.

An epitaxial relationship between $Cr_2O_3(0001)$ and corundum-phase TiO_2 -x(111), with similar lattice constants, is not surprising.

The existence of the observed exchange bias behavior (Fig. 6) would not be observed for a polycrystalline chromia layer [5], and is therefore corroborative evidence for an ordered chromia layer. Similar hysteresis curves, as seen in the MOKE of Figure 6, have been produced for strained Cr₂O₃(0001)/Al₂O₃(0001), but only in the polar (c-axis) direction [22]. In contrast, d⁰ ferromagnetism in rutile TiO₂ is manifested in-plane [5, 23]. Since the boundary layer magnetization of Cr₂O₃(0001) is oriented along the c-axis [24, 25], the observation of magnetic ordering by both planar (in the thin film plane) and polar (probing moment alignment along the normal) MOKE above and below the T_N for Cr₂O₃ indicates an interaction between the in-plane ferromagnetically ordered TiO_{2-x}(111) substrate and the polar-oriented boundary layer magnetization of the chromia. The off-center hysteresis in both the polar and planar MOKE (Fig. 6) is the characteristic signature of exchange bias in our Cr₂O₃/TiO₂-x interface. The exchange bias field for an AFM/FM interface is given by the Meiklejohn-Bean expression [26]:

$$\mu_o H_{EB} = -\frac{J S_{Cr_2O_3} S_{TiO_2}}{M_{TiO_2} t_{TiO_2}}$$
 (1)

where J is the phenomological coupling between d^0 ferromagnetism in rutile TiO₂ and boundary layer magnetization of the antiferromagnetic chromia. $S_{Cr_2O_3}$ and S_{TiO_2} are interface magnetizations, M_{TiO_2} is the saturation magnetization for ferromagnetic TiO₂ and t_{TiO_2} is the thickness of ferromagnetic layer. A hysteresis loop shift in planar MOKE data with an increase in temperature from 280 K to room temperature (not shown) also confirms the presence of exchange bias in the Cr_2O_3/TiO_{2-x} heterostructure. Similar hysteresis shifts along the direction of applied field have already been reported in the study of in-plane exchange bias of $Cr_2O_3(10-10)/rutile-TiO_2(001)$ interface [5]. In their study, they completely suppressed the perpendicular exchange bias by growing the Cr_2O_3 along the (10-10) plane, constraining the c-axis to lie in the film plane. For our study, we have grown Cr_2O_3 along the (0001) plane, and thus have seen a strong perpendicular exchange bias as shown in the polar MOKE data taken at 300 K Fig 6 (b). The presence of in-plane and perpendicular exchange bias is therefore evidence of interaction between the polar-oriented boundary layer magnetization of $Cr_2O_3(0001)$ and d^0 ferromagnetism of the $TiO_{2-x}(111)$ substrate, and compelling evidence that the actual spin structure is canted.

A pertinent question, particularly for device applications, is why this chromia interface exhibits exchange bias to above 300 K, yet a recently studied $Cr_2O_3(10-10)/TiO_2(001)$ interface [5] did not show such bias above ~ 40 K. In the absence of detailed knowledge of the chemistry of that interface, no firm conclusion is obtainable. An interesting possibility, however, is that the titania films examined here exhibited a significantly higher concentration of O vacancies than the rutile TiO_2 films examined by Yuan, et. al. [5]. The d^0 ferromagnetism of undoped TiO_2 and similar oxides has been correlated with O vacancies, and consequent n-type doping of the 3d conduction band [1, 3, 27]. Given the limited sensitivity of XPS to O vacancy formation, it may be that the titania Magnéli phase films examined here have higher concentrations of O vacancies than the more often examined rutile or anatase phases of TiO_2 . Magnéli phases are usually highly

conductive [28]. It may also be that formation of the interface in the manner reported here, resulting in significant additional oxygen vacancy formation in the TiO₂-x layer within the XPS sampling depth of the interface, may be responsible for the more thermally robust magnetic interactions reported here. In any case, the data reported here indicate that titania Magnéli phases are strong candidates for further study. Additionally, however, our data also suggest that Cr deposition under these conditions on, e.g., anatase or rutile TiO₂(001) or SrTiO₃(001) may result in sufficient titania O vacancy formation near the interface as to create a two-dimensional electron gas (2DEG) [29, 30]. The interaction of a magneto-electric antiferromagnet with such a two-dimensional electron gas as interesting device implications [4]. Such studies are in progress in our laboratories.

5. Summary and Conclusions

XPS, LEED, and EELS demonstrate that Ti MBE on $Al_2O_3(0001)$ at 500 K in 10^{-6} Torr O_2 yields corundum-phase TiO_2 -x(111) films for which $0 < x < \sim 0.3$. Subsequent deposition of Cr in UHV at room temperature results in $Cr_2O_3(0001)$ formation and additional Ti(III) formation within XPS sampling depth of the chromia/titania interface. Both planar and polar MOKE measurements indicate exchange bias characteristic of antiferromagnet/ferromagnet interaction, at temperatures up to at least 315 K. These results indicate that chromia/titania heterostructures with controlled oxygen vacancies in the titania phase exhibit significant potential for low power spintronic applications at and above room temperature.

Acknowlegements

Work at UNL was supported in part by the Semiconductor Research Corporation (SRC) as task 2760.002 and NSF through ECCS 1740136. Sebastian Engelmann and Scott Chambers are acknowledged for enlightening discussions.

References

- [1] T.C. Kaspar, S.M. Heald, C.M. Wang, J.D. Bryan, T. Droubay, V. Shutthanandan, S. Thevuthasan, D.E. McCready, A.J. Kellock, D.R. Gamelin, S.A. Chambers. Negligible magnetism in excellent structural quality $Cr_xTi_{1-x}O_2$ anatase: Contrast with high- T_c ferromagnetism in structurally defective $Cr_xTi_{1-x}O_2$. Phys. Rev. Lett. 95 (2005) 217203.
- [2] D. Kim, J. Jong, Y.R. Park, K.J. Kim. The origin of oxygen vacancy induced ferromagnetism in undoped TiO₂. J. Phys: Cond. Matt. 21 (2009) 195405.
- [3] A. Rumaiz K., B. Ali, A. Ceylan, M. Boggs, T. Beebe, S.I. Shah. Experimental studies on the vacancy induced ferromagnetism in undoped TiO₂. Sol. St. Commun. 144 (2007) 334-338.

- [4] P.A. Dowben, C. Binek, K. Zhang, L. Wang, W. Mei, J.P. Bird, U. Singisetti, X. Hong, K.L. Wang, D. Nikonov. Towards a strong spin-orbit coupling magnetoelectric transistor. IEEE J Exploratory Sol. -St. Computational Dev. and Circ. 4 (2018) 1-9.
- [5] W. Yuan, T. Su, Q. Song, W. Xing, Y. Chen, T. Wang, Z. Zhang, X. Ma, P. Gao, J. Shi, W. Han. Crystal structure manipulation of the exchange bias in an antiferromagnetic film. Sci Rep. 6 (2016) 28397.
- [6] A.B. Boffa, H.C. Galloway, P.W. Jacobs, J.J. Benitez, J.D. Batteas, M. Salmeron, A.T. Bell, G.A. Somorjai. The growth and structure of titanium oxide films on Pt(111) investigated by LEED, XPS, ISS and STM. Surf. Sci. 326 (1995) 80-92.
- [7] F. Sedona, G.A. Rizzi, S. Agnoli, Liabres i Xamena, Francesc X., A. Papageorgiou, D. Ostermann, M. Sambi, P. Finetti, K. Schierbaum, G. Granozzi. Ultrathin TiO_x films on Pt(111): A LEED, XPS and STM investigation. J Phys Chem B. 109 (2005) 24411-24426.
- [8] C. Breinlich, M. Bucholz, M. Moors, S. LeMoal, C. Becker, K. Wandelt. Scanning tunneling microscopy investigation of ultrathin titanium oxide films grown on Pt₃Ti(111). J. Phys. Chem. C. 118 (2014) 6186-6192.
- [9] O. Olanipekun, C. Ladewig, T. Estrada, J.A. Kelber, M.D. Randle, J. Nathawat, C. Kwan, J.P. Bird, P. Chakraborti, P.A. Dowben, T. Cheng, W.A. Goddard III. Epitaxial growth of cobalt oxide phases on Ru(0001) for spintronic device applications. Semicond, Sci. and Technol. 32 (2017) 095011.
- [10] S. Tanuma, C.J. Powell, D.R. Penn. Calculation of electron inelastic mean free paths (IMFPS) VII. reliability of the TPP-2M predictive equation: Surf. and Interf. Anal. 35 (2003) 268-275.
- [11] J.F. Moulder, W.F. Stickle, P.E. Soboland K.D. Bomben. Handbook of X-ray photoelectron spectroscopy. Physical Electronics, Eden Prairie, Minnesota, 1995.
- [12] M.P. Seah. Quantification of AES and XPS in M. P. Seah and D. Briggs (ed.) Practical surface analysis, second edition, volume 1-- auger and X-ray photoelectron spectroscopy vol., 86-255.
- [13] C.D. Wagner, A.V. Naumkin, A. Kraut-Vass, J.W. Allison, C.J. Powell, J.R.J. Rumble. "NIST standard reference database 20, version 3.4 (web version)" *Http://Srdata Nist Gov/Xps/*). (2003).
- [14] P. Weinberger. John Kerr and his effects found in 1877 and 1878. Philosph. Mag. Lett. 88 (2008) 897-907.
- [15] Y. Li, Y. Weng, X. Yin, X. Yu, S.R.S. Kumar, N. Wehbe, H. Wu, H.N. Alshareef, S.J. Pennycook, M.B.H. Bresse, J. Chen, S. Dong, T. Wu. Orthorohomic Ti₂O₃" A polymorph-dependent narrow-bandgap ferromagnetic oxide. Adv. Funct. Mater. 28 (2018) 1705657

- [16] X. Chen, H. Kazi, Y. Cao, B. Dong, F. Pasquale, J.A. Colon-Santan, S. Cao, M. Street, R. Welch, C. Binek, A. Enders, J. Kelber, P.A. Dowben. Ultrathin chromia films grown with preferential texture on metallic, semimetallic and insulating substrates. Mat. Chem. and Phys. 149-50 (2015) 113-123.
- [17] B. Bharti, S. Kumar, H. Lee, R. Kumar. Formation of oxygen vacancies and ti³⁺ sate in TiO₂ thin film and enhanced optical properties by air plasma treatment. Sci Rep. 6 (2016) 32355.
- [18] M.R. Bayati, R. Molaei, R.J. Narayan, J. Narayan, H. Zhou, S.J. Pennycook. Domain epitaxy in TiO_2/α -Al $_2O_3$ thin film heterostructures with Ti_2O_3 transient layer. Appl. Phys. Lett. 100 (2012) 251606
- [19] S.A. Chambers, M.H. Engelhard, L. Wang, T.X. Droubay, M.E. Bowden, M.J. Wahilia, N.F. Quackenbush, L.F.J. Piper, T. Lee, C.J. Nelin, P.S. Bagus. X-ray photoelectron spectra for single-crystal Ti₂O₃: Experiment and theory. Phys. Rev. B. 96 (2017) 205143.
- [20] S. Halpegamage, M. Batzill. Mixed oxide in rutile TiO₂(011): Cr₂O₃ and Cu₂O. J. Vac. Sci. and Technol. A. 35 (2017) 061406.
- [21] H. Sandamali, Z. Wen, X. Gog, M. Batzill. Monoalyer intermixed oxide surfaces: Fe, Ni, Cr and Va oxide on rutile TiO₂(011). J. Phys. Chem. C. 120 (2016) 14782-14794.
- [22] I. Tanabe, H. Kazi, Y. Cao, J.L. Rodenburg, T. Komesu, B. Dong, F.L. Pasquale, M.S. Driver, J.A. Kelber, P.A. Dowben. Strain induced super-paramagnetism in Cr₂O₃ in the ultra thin film limit. MRS Proc. 1729 (2015) http://dx.doi.org/10.1557/opl.2015.5.
- [23] N.H. Hong, J. Sakai, N. Poirot, V. Brize. Room-temperature ferromagnetism observed in undoped semiconducting and insulating oxide thin films. Phys. Rev. B. 73 (2006) 132404.
- [24] X. He, Y. Wang, N. Wu, A.N. Caruso, E. Vescovo, K.D. Belaschenko, P.A. Dowben, C. Binek. Robust isothermal electric control of exchange bias at room temperature. Nat. Mat. 9 (2010) 579-585.
- [25] N. Wu, X. He, A.L. Wysocki, U. Lanke, T. Komesu, K.D. Belashchenko, C. Binek, P. Dowben. Imaging and control of surface magnetization domains in a magnetoelectric antiferromagnet. Phys. Rev. Lett. 106 (2011) 087202.
- [26] W.H. Meiklejohn, C.P. Bean. New magnetic anisotropy. Phys. Rev. 105 (1957) 904-913.
- [27] T. Sarkar, K. Gopinadhan, J. Zhou, S. Saha, J.M.D. Coey, Y.P. Fen, Ariando, T. Venkatesan. Electron transport at the TiO₂ surfaces of rutile, anatase and strontium titanate: The influence of orbital corrugation. ACS Appl. Mater. Interf. 7 (2015) 24616-24621.
- [28] A.F. Arif, R. Balgis, T. Ogi, F. Iskandar, A. Kinoshita, K. Nakamura, K. Okuyama. Highly conductive nano-sized Magnéli phases in titanium dioxide (TiO_x). Sci Rep. 7 (2017) 3646.

- [29] T.C. Rödel, F. Fortuna, F. Bertran, M. Gabay, M.J. Rozenberg, A.F. Santander-Syro, P. LeFevre. Engineering two-dimensional electron gases at the (001) and (101) surfaces of TiO₂ anatase using light. Phys Rev B. 92 (2015) 041106(R).
- [30] C. Li, Y. Hong, H. Xue, X. Wang, Y. Li, K. Liu, W. Jiang, M. Liu, L. He, R. Dou, C. Xiong, J. Nie. Formation of two-dimensional electron gas at amorphous/crystalline oxide interfaces. Sci Rep. 8 (2018) 404.

Figures and Captions

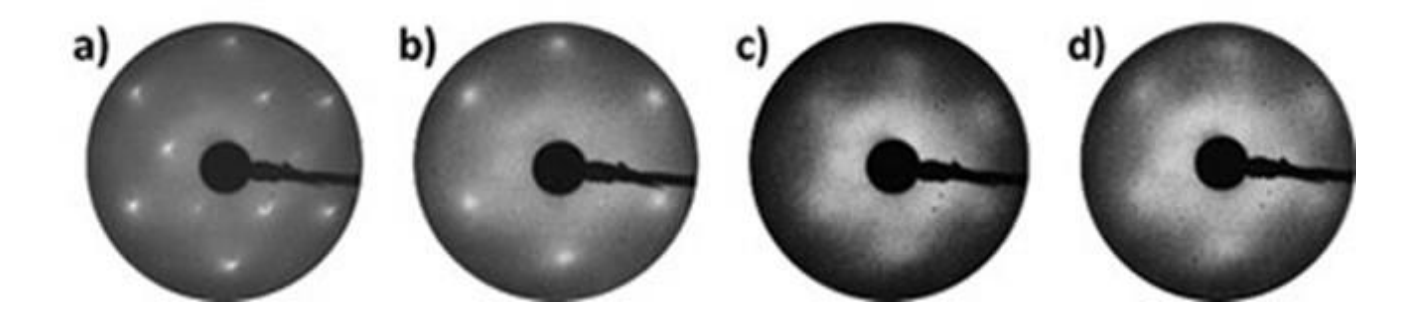


Fig. 1 LEED images of (a) a clean $Al_2O_3(0001)$ substrate; (b) a 49 Å thick $TiO_{1.8}(111)$ film deposited on $Al_2O_3(0001)$; (c) a similar film as in (b) but annealed at 1000 K in 10^{-6} Torr O_2 for 300 min; (d) after deposition of Cr and formation of ~ 10 Å of chromia. The images were acquired at 60 eV (a,b), 100 eV (c) and 80 eV electron beam energy due to significant sample charging.

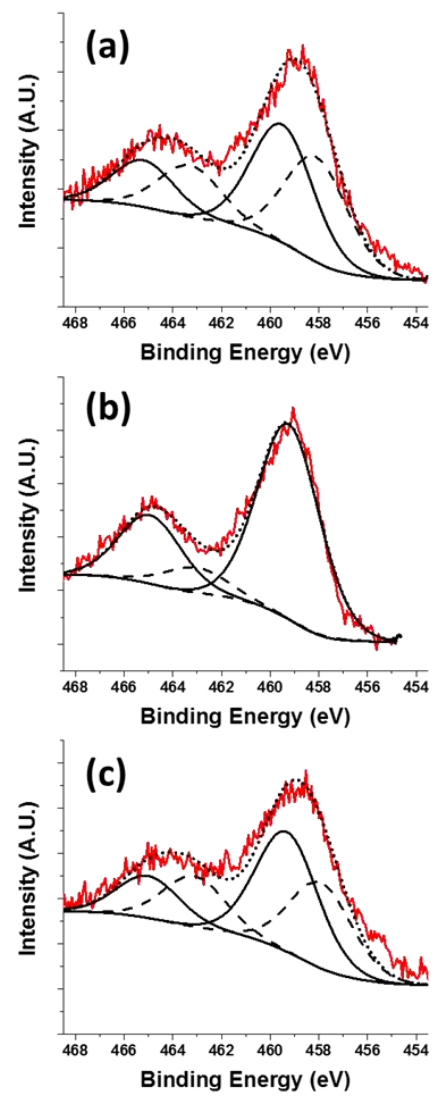


Fig. 2 XPS Titanium oxide spectra (a) TiO_{1.7}(111) film (as in Fig. 1b); (b) Nearly stoichiometric film obtained after annealing in 10⁻⁶ Torr O₂ for 300 min (as in Fig. 1c); and (c)after Cr deposition at room temperature (as in Fig. 1d). Red trace—experimental spectrum; solid black trace—Ti(IV) component; dashed black trace—Ti(III) component; dotted trace—sum of Ti(IV) and Ti(III) components.

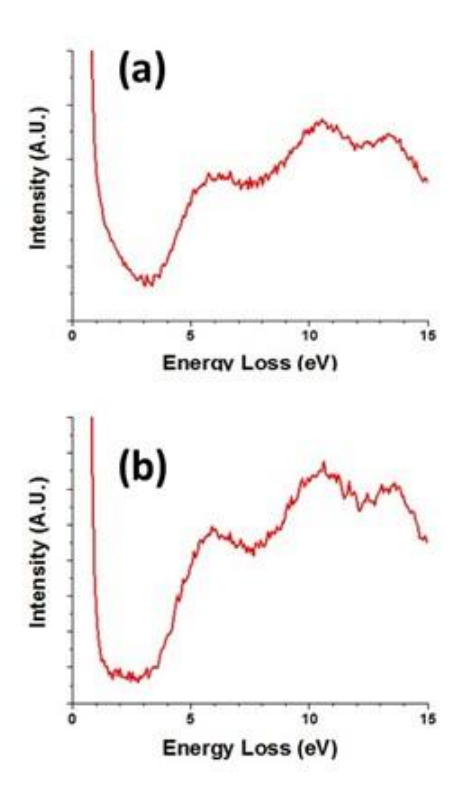


Figure 3. EELS spectra for 5 nm thick titania film (a) after Ti deposition ((5) in Fig. S1) and annealing in O_2 ((6) in Fig. S1). Electron excitation energy is 100 eV.

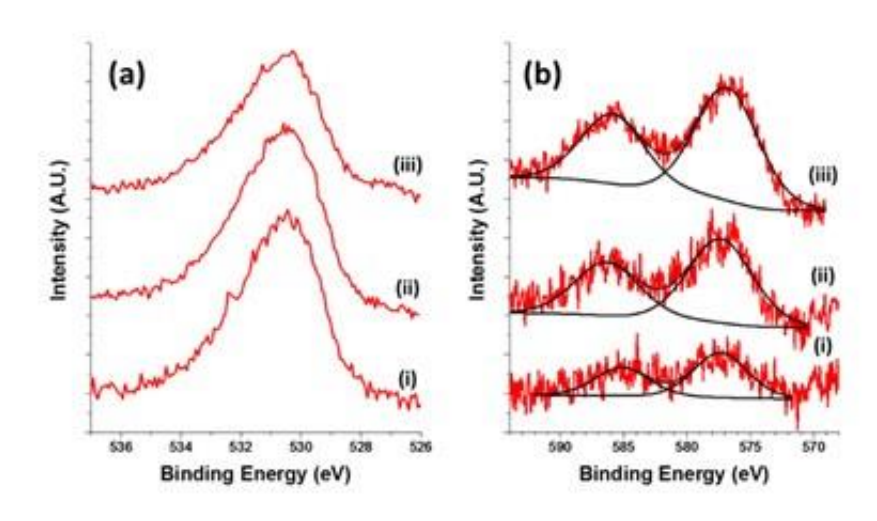


Figure 4. Evolution of (a) O 1s) and (b) Cr 2p spectra upon Cr deposition for average Cr thicknesses of (i) 2.1 Å, (ii) 6.6 Å and (iii) 10 Å.

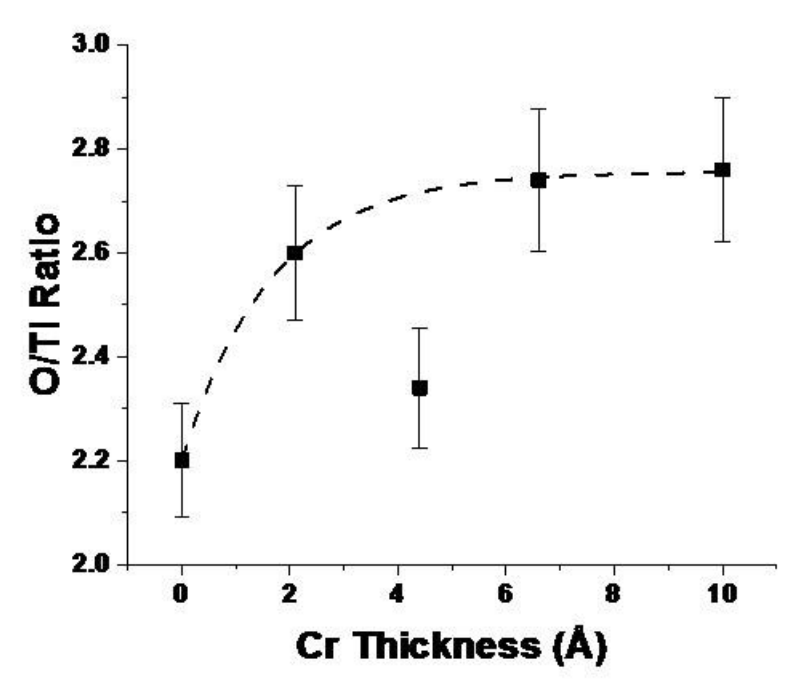


Figure 5 O 1s/Ti 2p XPS intensity ratio as a function of chromia overlayer deposition at room temperature. Dashed line is an exponential fit to the data, excluding the data point near $4\,\text{Å}$ Cr thickness.

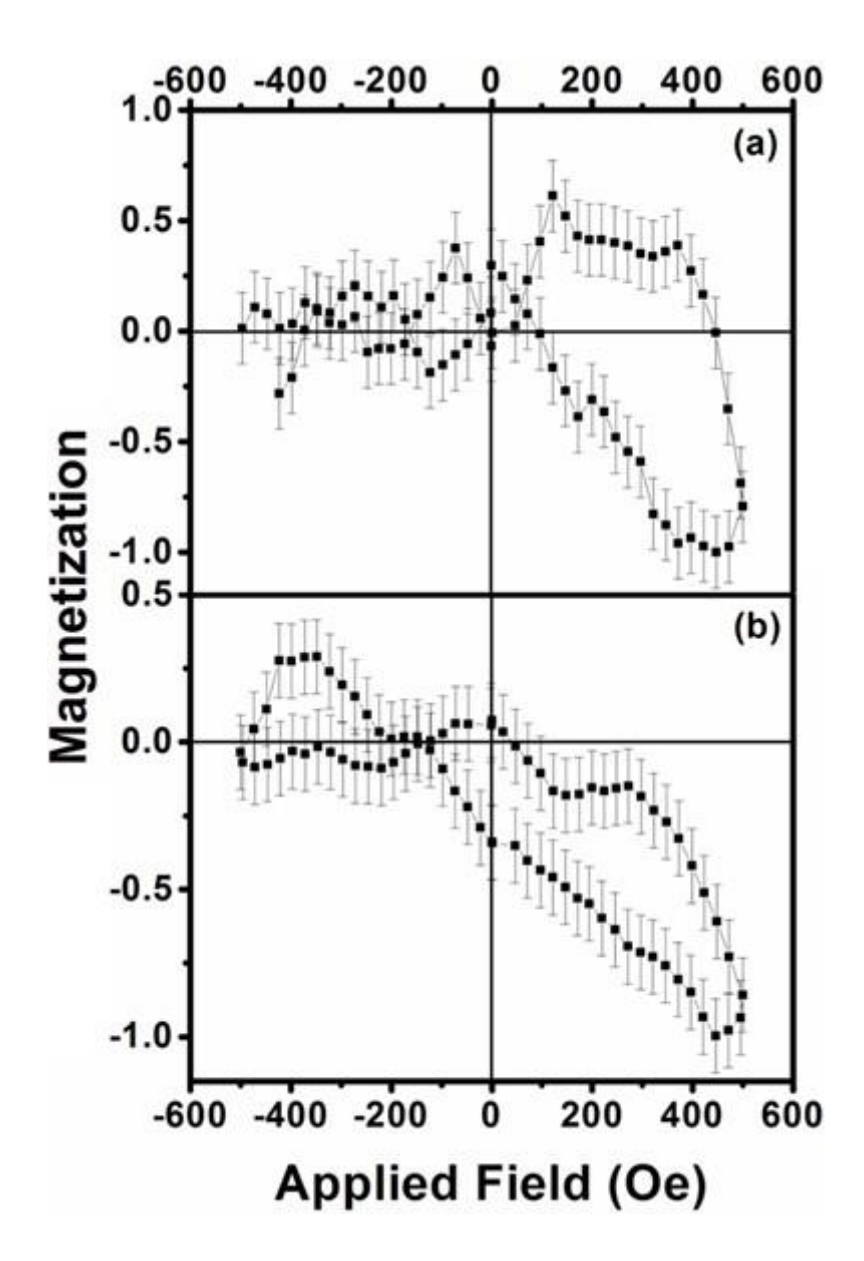


Figure 6. (a) Planar MOKE data and (b) Polar MOKE data, acquired at 300 K for the same film as in Figs. 4 and 5. Similar planar MOKE data were obtained at 280 K - 315 K.